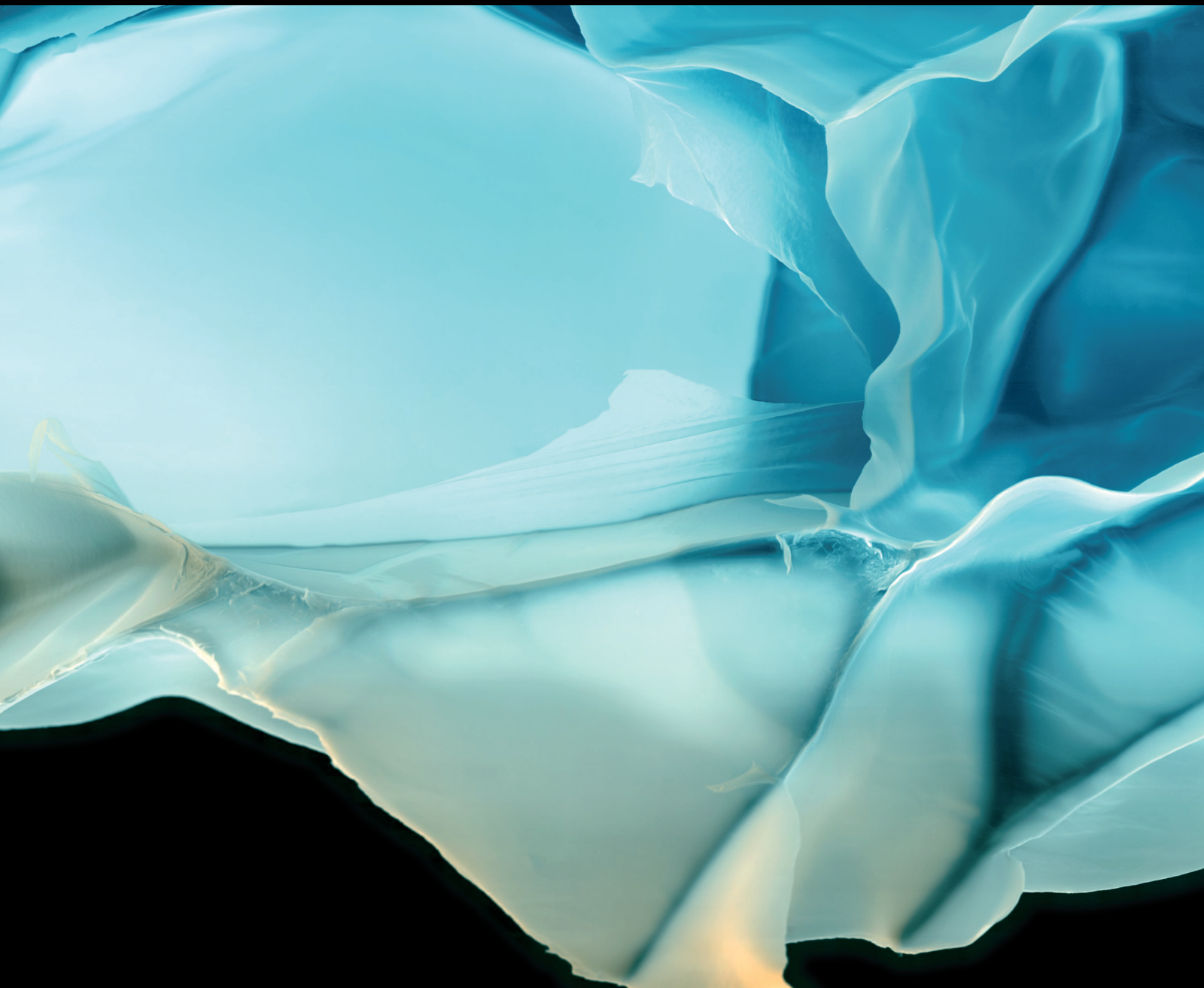


Conducting Polymers for Technological Advances

Lead Guest Editor: Arunas Ramanavicius

Guest Editors: Inga Morkvenaite-Vilkonciene, Urte Samukaite-Bubniene, Simonas Ramanavicius, Roman Viter, and Igor Iatsunskiy





Conducting Polymers for Technological Advances

Advances in Polymer Technology

Conducting Polymers for Technological Advances

Lead Guest Editor: Arunas Ramanavicius

Guest Editors: Inga Morkvenaite-Vilkonciene,
Urte Samukaite-Bubniene, Simonas Ramanavicius,
Roman Viter, and Igor Iatsunskyi



Copyright © 2023 Hindawi Limited. All rights reserved.

This is a special issue published in "Advances in Polymer Technology." All articles are open access articles distributed under the Creative Commons Attribution License, which permits unrestricted use, distribution, and reproduction in any medium, provided the original work is properly cited.

Chief Editor

Ning Zhu , China

Associate Editors

Maria L. Focarete , Italy
Leandro Gurgel , Brazil
Lu Shao , China

Academic Editors

Nasir M. Ahmad , Pakistan
Sheraz Ahmad , Pakistan
B Sridhar Babu, India
Xianglan Bai, USA
Lucia Baldino , Italy
Matthias Bartneck , Germany
Anil K. Bhowmick, India
Marcelo Calderón , Spain
Teresa Casimiro , Portugal
Sébastien Déon , France
Alain Durand, France
María Fernández-Ronco, Switzerland
Wenxin Fu , USA
Behnam Ghalei , Japan
Kheng Lim Goh , Singapore
Chiara Gualandi , Italy
Kai Guo , China
Minna Hakkarainen , Sweden
Christian Hopmann, Germany
Xin Hu , China
Puyou Jia , China
Prabakaran K , India
Adam Kiersnowski, Poland
Ick Soo Kim , Japan
Siu N. Leung, Canada
Chenggao Li , China
Wen Li , China
Haiqing Lin, USA
Jun Ling, China
Wei Lu , China
Milan Marić , Canada
Dhanesh G. Mohan , United Kingdom
Rafael Muñoz-Espí , Spain
Kenichi Nagase, Japan
Mohamad A. Nahil , United Kingdom
Ngoc A. Nguyen , USA
Daewon Park, USA
Kinga Pielichowska , Poland

Nabilah Afiqah Mohd Radzuan , Malaysia
Sikander Rafiq , Pakistan
Vijay Raghunathan , Thailand
Filippo Rossi , Italy
Sagar Roy , USA
Júlio Santos, Brazil
Mona Semsarilar, France
Hussein Sharaf, Iraq
Melissa F. Siqueira , Brazil
Tarek Soliman, Egypt
Mark A. Spalding, USA
Gyorgy Szekely , Saudi Arabia
Song Wei Tan, China
Faisal Amri Tanjung , Indonesia
Vijay K. Thakur , USA
Leonard D. Tijing , Australia
Lih-sheng Turng , USA
Kavimani V , India
Micaela Vannini , Italy
Surendar R. Venna , USA
Pierre Verge , Luxembourg
Ren Wei , Germany
Chunfei Wu , United Kingdom
Jindan Wu , China
Zhenhao Xi, China
Bingang Xu , Hong Kong
Yun Yu , Australia
Liqun Zhang , China
Xinyu Zhang , USA

Contents

Removal of Dye from Wastewater Using a Novel Composite Film Incorporating Nanocellulose

Ismat Ara Eti, Marufa Khatun, Most. Afroza Khatun, Md. Owaleur Rahman, K. M. Anis-Ul-Haque, and Md. Jahangir Alam 

Research Article (9 pages), Article ID 4431941, Volume 2023 (2023)

Research Article

Removal of Dye from Wastewater Using a Novel Composite Film Incorporating Nanocellulose

Ismat Ara Eti,¹ Marufa Khatun,¹ Most. Afroza Khatun,¹ Md. Owaleur Rahman,¹ K. M. Anis-Ul-Haque,² and Md. Jahangir Alam ¹

¹Department of Chemical Engineering, Jashore University of Science and Technology, Jashore 7408, Bangladesh

²Department of Chemistry, Jashore University of Science and Technology, Jashore 7408, Bangladesh

Correspondence should be addressed to Md. Jahangir Alam; jahangirche@gmail.com

Received 17 July 2022; Revised 27 October 2022; Accepted 24 November 2022; Published 20 January 2023

Academic Editor: Arunas Ramanavicius

Copyright © 2023 Ismat Ara Eti et al. This is an open access article distributed under the Creative Commons Attribution License, which permits unrestricted use, distribution, and reproduction in any medium, provided the original work is properly cited.

Research shows that the composite material is used as an adsorbent to remove pollutants from wastewater. This work is aimed at producing a novel composite film comprising chitosan, polyvinyl alcohol, and cornstarch incorporating nanocellulose (CPCN). The composite film was prepared by a blending method wherein nanocellulose was extracted using a chemical method from banana bract. The prepared CPCN was characterized using Fourier-transform infrared spectroscopy (FTIR) and scanning electron microscopy (SEM) with EDX to understand their molecular interaction and surface morphology, respectively. The effect of parameters including pH, adsorbent dosage, initial dye concentration, and contact time on the adsorption of methylene blue (MB) dye was studied. The maximum adsorption was found to be up to 63.13 mg/g MB with a pH of 10, adsorbent dosage of 2 g, an initial concentration of 150 ppm, and contact time of 120 min at room temperature (25°C) indicating a moderate adsorption capacity of the CPCN. Comparing the Langmuir and Freundlich adsorption isotherm models, the former fitted well with MB dye adsorption data, implying that the models can be applied to uptake MB dye by CPCN. In the kinetic adsorption experiment, the adsorbed dye almost reached equilibrium at about 120 min for the CPCN and followed the pseudo-second-order kinetic model. Therefore, the CPCN can be used as a potential adsorbent in wastewater treatment.

1. Introduction

Recently, the highly polluting nature of conventional plastic films compelled scientists to consider the development of novel edible composite films [1]. The capacity of biopolymer-based conductive polymer composites (CPCs) to increase the shelf life or enhance the safety of food would open up numerous opportunities for active packaging in the food packaging industry [2, 3]. In addition, these kinds of materials can also be used as adsorbents in biological applications such as biosensors [4], drug delivery systems, neural electrodes, and bioactuators [5], as well as in wastewater treatment [6, 7], and water quality measurement [8]. Chitosan is a type of chitin that occurs naturally in the exoskeletons of crustaceans and contains a few acetyl groups. It is the second most abundant natural biopolymer by volume. Chitosan is a great film-forming material with outstanding gas permeability and cov-

ered mechanical properties, as well as being biodegradable, nontoxic, and exhibiting significant antibacterial and antifungal activity and low oxygen and carbon dioxide permeability [9–11]. The PVA is a biopolymer with unique qualities such as excellent moisture absorption, fiber formability, biocompatibility, chemical tolerance, biodegradability, and swelling properties. It is a copolymer of vinyl alcohol and vinyl acetate [12]. Cornstarch, a natural, affordable, and biodegradable polymer, has long been used as a substitute for synthetic polymers generated from petroleum [13]. It is derived from the endosperm of the kernel and typically consists of 27% amylose and 73% amylopectin.

On the other hand, nanomaterial attained from plant resources with various application forecasts has attracted significant attention. Nanocellulose is the natural fiber extracted from cellulose, the main structural component of plant cell walls. This material (nanocellulose) shows promise

as a novel category of reinforcing filler in the field of composite materials. It is also gleaming, conducts electricity, and is more durable than steel [14–17]. Banana bract (BB) is available in agricultural residues worldwide for the source of cellulose with a nanostructure and has been used in different applications. As a source of nanocellulose, it is attracting attention in degradable antimicrobial composite films preparations for food packaging, as an adsorbent for wastewater purification, and other applications. Over the last few decades, research into the production of biodegradable composite materials from renewable sources has increased interest in biocomposites made from various natural fibers. BB is a fiber extracted from the banana inflorescence, a lustrously colored, spirally arranged, boat-shaped spathe. It consists of cellulose 56.48%, hemicellulose 14.03%, ash 1.3%, and other components 28.44% [18]. The cellulose from BBs can be easily obtained by bleaching and alkali treatment, along with nanocellulose obtained from acid hydrolysis of cellulose.

The composite film can be produced by physical blending and chemical cross-linking of different polymers. The later polymer blending is an effective method to bestow the desired novel composite films [19]. The composite product of synthetic polymers and biopolymers to attain the desired properties has become of utmost interest to researchers. Several studies have been performed to produce composite films for various applications. Noorbakhsh-Soltani et al. [20] (2018) present the gelatin- and starch-based nanocomposite film incorporating nanocellulose. Another composite film was prepared with chitosan/cellulose acetate phthalate incorporated with ZnO nanoparticles [21]. Zhou et al. [22] (2021) produced a sustainable composite film with corn starch/cellulose nanofibrils that were incorporated into biodegradable polyvinyl alcohol through melt processing. This study presents the preparation of chitosan/PVA/cornstarch/nanocellulosic novel composite films. So far, we know, in the literature, there is no same combination of polymers to produce the composite film. In contrast, this study proposes an alternative method to remove methylene blue dye by CPCN from industrial wastewater. The surface morphology and molecular interaction of CPCN were investigated by scanning electron microscopy (SEM) and Fourier-transform infrared spectroscopy (FTIR), respectively. From the moderate capacity of CPCN to remove MB, it can be proposed as a potential adsorbent to remove organic dyes from industrial wastewater.

2. Materials and Methods

2.1. Materials. Raw banana bract was collected from the local area of Jashore, Bangladesh. Sisco Research Laboratories Pvt Ltd., India, has supplied chitosan with a degree of deacetylation of 90%. Food grade cornstarch (CS) was purchased from Yong Wen Holdings SDN BHD, Malaysia, and polyvinyl alcohol (PVA) was purchased from the Laboratory of Advanced Technology Innovation, USA. Sodium hydroxide, sodium chloride, and sulfuric acid were procured from Merck, Germany. All chemicals were of analytical grade and used as received.

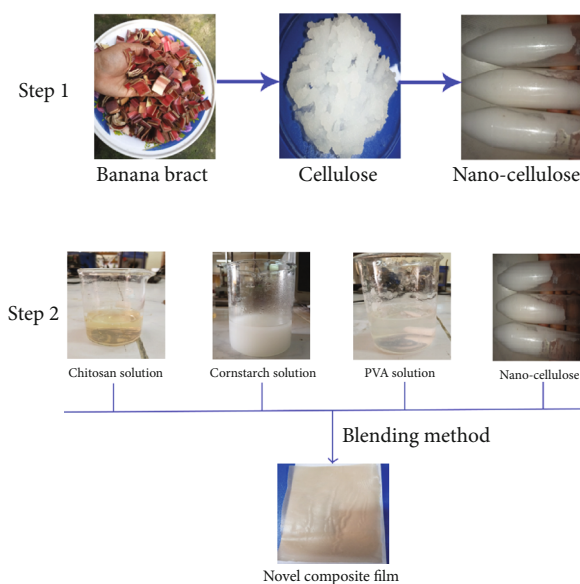


FIGURE 1: Physical view of novel composite film preparation.

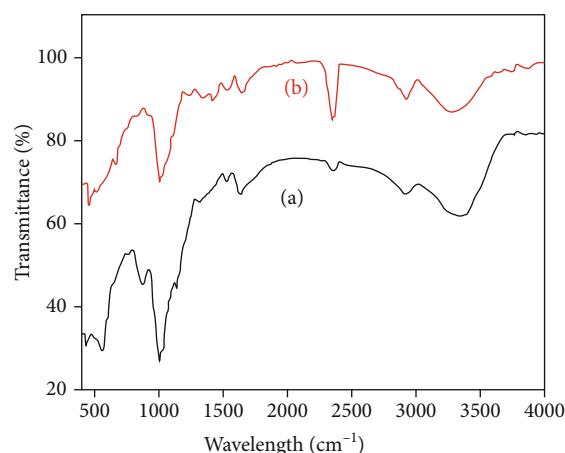


FIGURE 2: FTIR spectra of CPCN film (a) before and (b) after adsorption.

2.2. Preparation of Cellulose and Nanocellulose. Raw banana bract was washed, dried, ground, and stored as powder form in an air-tight bag. Cellulose was extracted from banana bracts via delignification with sodium hydroxide, followed by bleaching with sodium chlorite. The cellulose was then hydrolyzed by sulfuric acid to prepare nanocellulose. The addition of distilled water stopped the hydrolysis reaction. The nanocellulose suspension was washed several times with distilled water, followed by centrifugation until neutral pH. Finally, the nanocellulose suspension was kept in a sealed glass vial in the refrigerator.

2.3. Preparation of Composite Films. Firstly, 2 g of chitosan was dissolved in 100 ml aqueous solution of acetic acid (2%, g/v), and 0.5% glycerol (g/v) was also added to the solution as a plasticizer. PVA and cornstarch solutions were prepared separately by dissolving 4 g of PVA/cornstarch in 100 ml of distilled water. The sonication of the solution

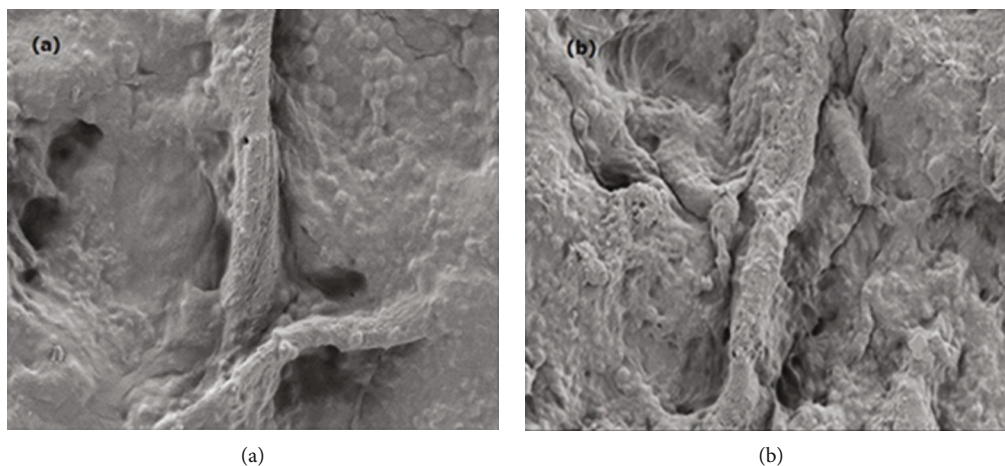


FIGURE 3: SEM image of the prepared CPCN composite film (a) before and (b) after adsorption.

was performed for 30 min to remove bubbles. Chitosan/cornstarch/PVA composite films were prepared by blending them at a volume ratio of 80:80:40 with incorporating 2 g nanocellulose. The mixture was continuously stirred for 20 min at 30°C to get a homogenous mixture. Then, the prepared mixture was poured into a silicon cloth-covered glass plate (9" × 6") and dried at 40°C until dry. After complete drying, the film was cooled at room temperature and removed from the plate. The physical view of the novel composite film preparation is shown in Figure 1.

2.4. Apparatus. UV-Vis spectrophotometer (model: GENESYS™ 150, supplied by Thermo Fisher Scientific, USA) to measure the concentration of dye, Fourier-transform infrared spectrophotometer (FTIR) (model: AIM-8800, supplied by SHIMADZU, Japan), and scanning electron microscopy (SEM) (model: JSM-6490, JEOL, Japan) were employed for sample characterization to understand the molecular interaction and surface morphology of them.

2.5. Determination of Methylene Blue Dye Adsorption. The batch adsorption experiments of MB on the composite film of CPCN were studied to measure the effect of pH, initial dye concentration, adsorbent dose, and time using a UV-visible spectrophotometer. A stock solution of methylene blue of 100 ppm was prepared and more diluted to the chosen concentration. For the individual experiment, in a 30 ml MB dye solution, a known amount of the adsorbent (films) was taken. The dye concentration in the solution was experienced using a UV spectrophotometer at 665 nm. After each experiment was done under similar conditions, the average values were calculated. The absorption capacity of CPCN was determined for methylene blue adsorption as follows [23–27]:

$$\text{Dye absorption capacity} = \frac{L(C_1 - C_2)}{M}, \quad (1)$$

where L is the volume of the dye solution in liter, M is the weight of CPCN in g, C_1 is the concentration of dye solution

before adsorption, and C_2 is the concentration of dye solution after adsorption.

3. Results and Discussions

3.1. FTIR Analysis. According to Figures 2(a) and 2(b), a strong band before adsorption appeared at 3391 cm⁻¹ (became more potent due to the addition of nanocellulose), and 3306 cm⁻¹ appeared after adsorption indicates -OH or N-H stretching. The peak at 2925 cm⁻¹ before and after adsorption resembled the C-H stretching. Physical blends vs. chemical interactions are accompanied by variations in typical spectrum peaks when two or more substances are mingled. The peak belonging to the -OH group, which overlays the NH stretching in the same region, becomes extensive and shifts to lower bands when the chitosan concentration is more excellent annual, suggesting that the chitosan addition reduces the hydrogen bonding interaction in PVA film [9]. The peak located at 1540 cm⁻¹ was the indication of NH bending (amide II). The peak located at 1653 cm⁻¹ due to the C=O (amide I) when NC added to the film. The peaks at 2924 cm⁻¹ and 847 cm⁻¹ show the presence of C-H symmetrical stretching and the C-N bending of MB. The extra band at 572 cm⁻¹ could be due to adsorbent/adsorbate interaction, confirming the cationic MB dye adsorption on the surface of the adsorbent [28].

3.2. SEM Analysis. The morphology of the prepared composite film was observed by SEM as exhibited in Figure 3. All these composite films exhibited dense and nonporous structures that are similar phenomena to PVA-based films in other works. From Figure 3(a), there was the presence of some wrinkles and fibers on the surface of CPCN film, which broke the original tight and orderly structure of the composite films. A parallel phenomenon originated in the study of reviews on the properties and challenges of cellulose nanocrystals and related nanocomposites [29]. Therefore, the interaction between nanocellulose and polymers might make a stable phenomenon of CPCN film. On the other hand, Figure 3(b) shows the morphology after MB adsorption by the prepared composite film. The CPCN film with

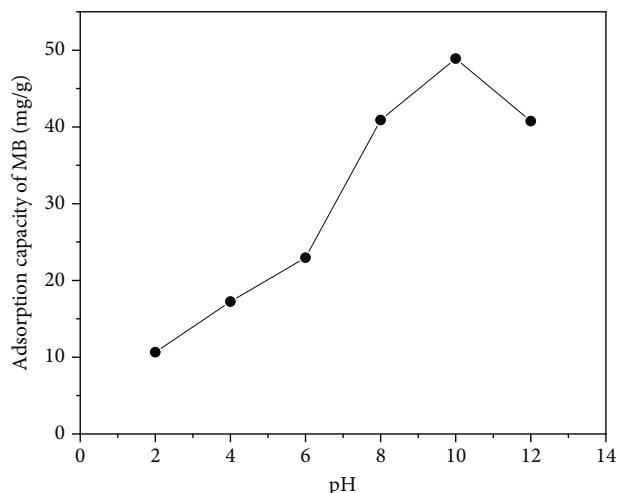


FIGURE 4: Effect of pH on removal of MB (adsorbent dosage 2 g, initial concentration 100 ppm, and contact time 60 min).

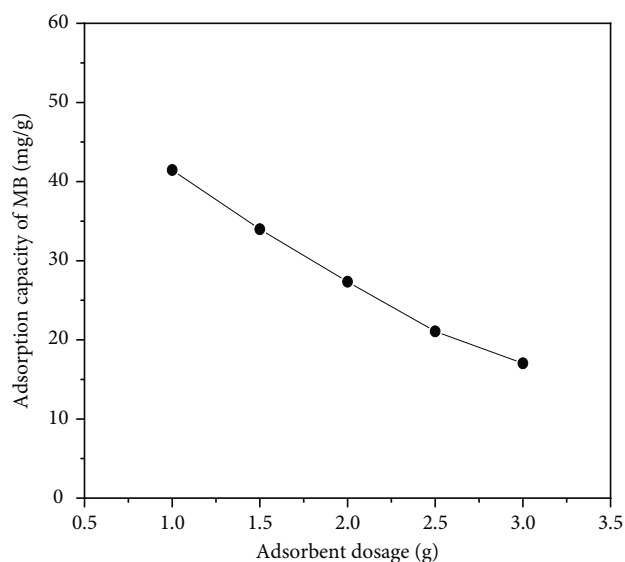


FIGURE 5: Effect of adsorbent dosage on removal of MB (pH 10, initial concentration 100 ppm, and contact time 60 min).

adsorbed MB dye exhibits a cylindrical rod-like shape with a slightly rough surface, associated with heterogeneous pore distribution through its matrix, meaning MB is adsorbed on the surface. The EDX analysis results further proved MB dye adsorption on the surface of CPCN-prepared composite film. The increased amount of sulfur, sodium, and chlorine in the prepared CPCN composite film after adsorption showed owing to the MB adsorption onto the adsorbent surface.

3.3. Effect of pH. The pH of the solution has essential effects on the adsorbent as the stability of the dyed surface. The effect of solution pH on methylene blue removal is presented in Figure 4. The adsorbent (composite film) used in this study has shown high dye removal ability in the solution pH at 10. At this pH, the prepared CPCN composite film

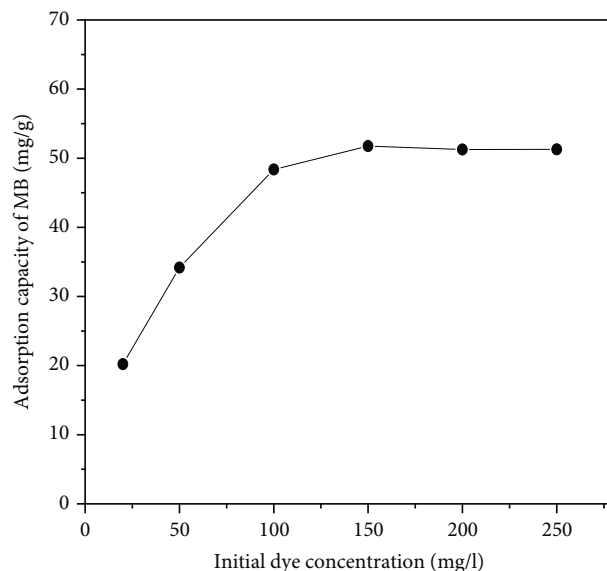


FIGURE 6: Effect of initial dye concentration on removal of MB (pH 10, adsorbent dosage 2 g, and contact time 60 min).

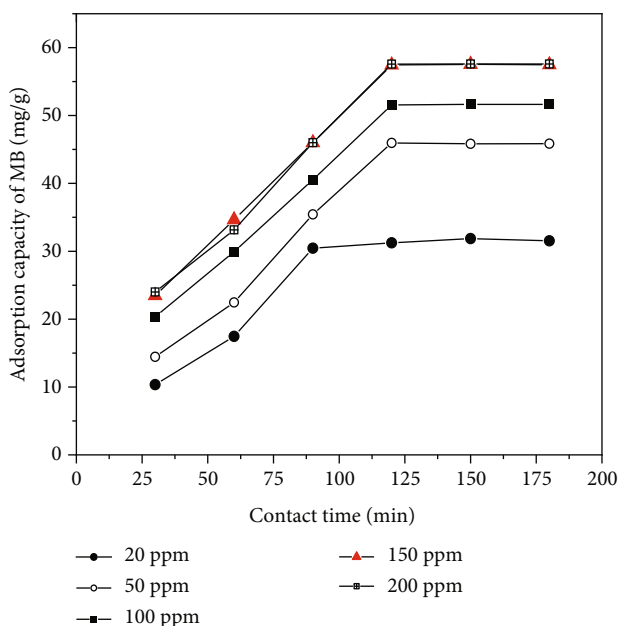


FIGURE 7: Effect of contact time on the removal of MB (pH 10, adsorbent dosage 2 g, and initial dye concentration 150 ppm).

showed the highest removal amount of dye at 48.90 mg/g. A similar influence of pH on methylene blue adsorption onto activated carbon/cellulose biocomposite films was studied in the open literature [30]. In an acidic environment, the positively charged surface of the adsorbent produces a repulsive force between cationic methylene blue and the positively charged surface of the adsorbent. The adsorbent becomes negatively charged in the alkaline pH value as MB cation effectively adsorbed onto the adsorbent surface. This result was in agreement with the study reported by Salama et al. [31] on the removal of MB on oxidized cellulose-reinforced silica gel.

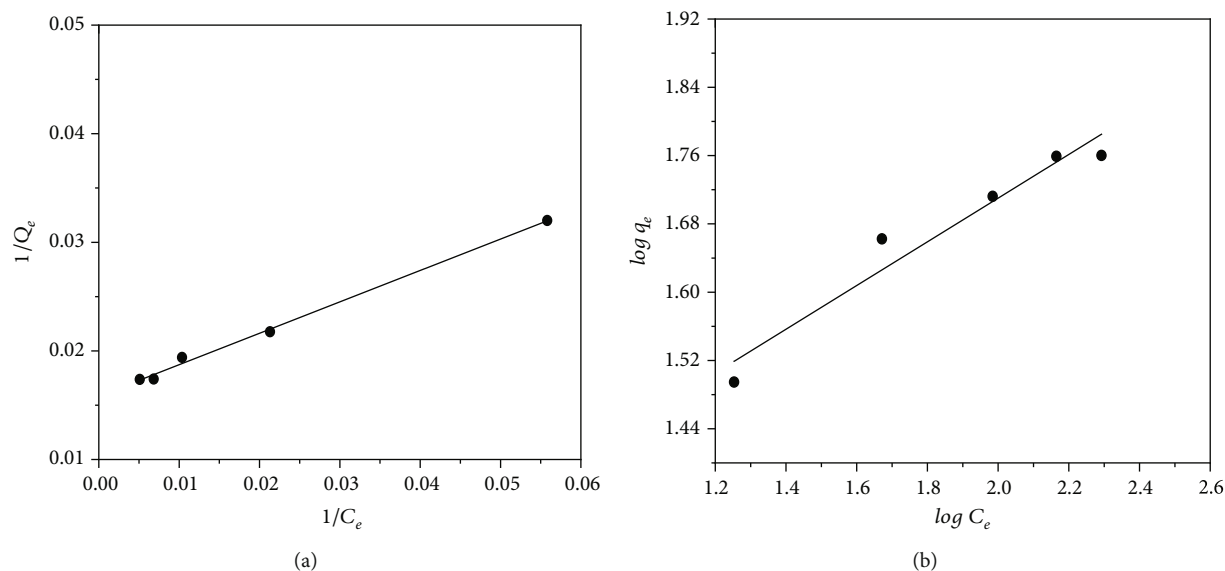


FIGURE 8: Adsorption isotherm models: (a) Langmuir and (b) Freundlich.

3.4. Effect of Adsorbent Dosage. The adsorption of MB on CPCN composite film was investigated by varying the amount from 1 to 3 g of adsorbent dosage in the test solution while maintaining the initial MB concentration of 100 ppm and pH 10 at contact periods of 60 min. According to Figure 5, with increasing adsorbent dosage from 1 to 3 g, the MB adsorption capacity decreased from 41.46 to 17.03 mg/g. As the adsorbent dose of 2 g, the highest amount 54.7 mg MB was removed by CPCN film. At a low level of adsorbent dosage, the adsorption sites were fully available for MB adsorption, resulting in a higher capacity. When the adsorbent dose increases, the particles agglomerate, affecting the surface area. As a result, active adsorbent sites become saturated, triggering a low adsorption capacity of a high adsorbent dose composite [32].

3.5. Effect of Initial Dye Concentration. The initial dye concentration significantly impacts the proportion of dye removal. Based on the linear relationship between dye concentration and accessible binding sites on an adsorbent surface, the initial dye concentration factor has an influence. The effect of initial dye concentration on adsorption capability was investigated in the range of 20 to 250 ppm at pH 10, adsorbent dosage 2 g, and contact time 60 min that is shown in Figure 6. At 150 ppm, the prepared CPCN composite film gave the highest adsorption capacity of 51.75 mg/g. Then, it decreases slightly when the concentration increases because, firstly, more dye can bind on the usable adsorbent surface, and then, the saturation of the surface active site makes it constant. Initially, as the dye concentration rises, the driving force for mass transfer rises, resulting in increased MB adsorption. Increased MB concentration results in more dye molecules, resulting in a longer contact time between the active site over the adsorbent and the adsorbate, resulting in saturation and a reduction in adsorption capacity [33].

TABLE 1: Isotherm parameters for methylene blue adsorption onto the prepared CPCN composite film.

Model	Parameters				R^2
	q_{\max} (mg/g)	K_b (l/mg)	K_F (l/mg)	n	
Langmuir	63.13	0.055			0.995
Freundlich			15.78	3.91	0.976

3.6. Effect of Contact Time. The relationship between MB removal and contact time has been investigated in this study. Figure 7 shows the adsorption capacity of MB concerning different contact times of 30 to 180 min at pH 10, an adsorbent dosage of 2 g, and an initial dye concentration of 150 ppm. As the time increases, more dye is adsorbed until a saturation point. The adsorption capacity increases from 31.34 to 57.44 mg/g with increasing initial concentration (20 to 200 ppm) of MB at a contact time 120 min. Increasing initial concentration of MB leads to the construction of sorbate-sorbate associations that provides the driving force to overcome the resistance to the mass transfer owing to increased adsorption. The MB removal capacity was highest at about 57.44 mg/g at 150 ppm with 120 min contact time. An optimum contact time to occupy the active site over the adsorbent and adsorbate led to saturation; hence, the adsorption capacity will not increase [34].

3.7. Adsorption Isotherm. The CPCN composite film adsorption properties were investigated by submerging the sample in MB at different concentrations from 20 to 250 mg/l at pH 10 for 120 min with a 2 g adsorbent dosage. The Langmuir isotherm model describes the information for the adsorption of MB dye onto the surface of composite films adsorbent homogeneously, and the dye molecule formed a monolayer at the adsorption sites. The Freundlich isotherm model predicts that nonideal multilayer adsorption occurs on the adsorbent's uneven surface and that the adsorbent's surface is heterogeneous. The Langmuir and Freundlich

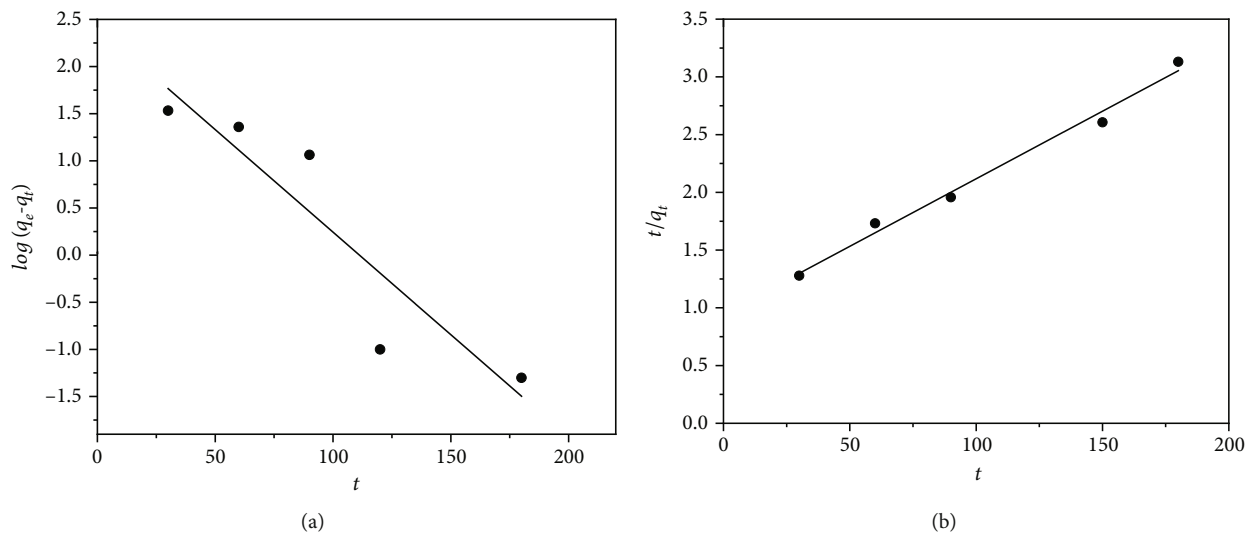


FIGURE 9: Adsorption kinetics: (a) pseudo-first-order model and (b) pseudo-second-order model.

models were applied to explain the equilibrium adsorption isotherm. Since this information can connect the adsorbate and adsorbent, the surface and adsorbate might adhere via chemisorption or physisorption. The linearized form of the Langmuir isotherm Equation (2) and Freundlich isotherm Equation (3) can be given by the following equation [35].

$$\frac{1}{q_e} = \frac{1}{q_{\max}} + \frac{1}{K_b q_{\max} C_e}, \quad (2)$$

where q_e is the amount of adsorbate adsorbed per unit weight of adsorbent at equilibrium (mg/g), C_e indicates the dye concentration in the equilibrium solution (mg/l), q_{\max} is the maximum adsorption capacity, and K_b is the adsorption equilibrium constant (l/mg).

The Freundlich isotherm can be expressed as follows:

$$\log q_e = \log K_F + \frac{1}{n} \log C_e, \quad (3)$$

where K_F is the affinity of the adsorbate towards the adsorbent (l/mg) and $1/n$ is the adsorption intensity or surface heterogeneity.

Figure 8 shows the linearized Langmuir and Freundlich isotherm plots. The calculated values of the parameters and the coefficient of determination (R^2) of these isothermal adsorption models are listed in Table 1. The analyzed results showed that the higher R^2 value indicates the Langmuir model was better fitted than the Freundlich model for MB dye adsorption by CPCN composite film, specifying that the adsorption behavior was better described by the Langmuir isotherm. Hence, the methylene blue molecules were adsorbed on the film surface as monolayer adsorption and give an adsorption capacity around 63.13 mg/g. Similar results of the correlation coefficient of adsorption isotherms were observed [12].

3.8. Adsorption Kinetics. The study of kinetics was a beneficial tool to inspect the adsorption rate and provide the sorp-

tion mechanism. The adsorption kinetic phenomena of cationic MB dye by the prepared CPCN composite film adsorbent are presented in Figure 9. The experiment data were plotted to fit the pseudo-first-order (PFO) and pseudo-second-order (PSO) equations of kinetics which are presented in the following manner, respectively [36–39]. The linear form of the first-order kinetic model is expressed as follows.

$$\text{Log}(q_e - q_t) = \text{Log}q_e - \frac{k_1}{2.303} t, \quad (4)$$

where q_e is the amount of dye adsorbed on the adsorbent at equilibrium and q_t is the amount of dye adsorbed on the adsorbent at any time, $k_1 =$ rate constant (min^{-1}). q_e and k_1 can be obtained by the intercept and slope of the plot of $\log(q_e - q_t)$ against t . In addition, the pseudo-second-order kinetic equation is expressed as follows.

$$\frac{t}{q_t} = \frac{1}{k_2 q_e^2} + \frac{1}{q_e} t, \quad (5)$$

where k_2 is the pseudo-second-order rate constant (min.g/mg) and q_e and q_t represent the amount of dye adsorbed (mg/g) at equilibrium and at time t .

Figures 9(a) and 9(b) display the linearized graphs of pseudo-first-order and pseudo-second-order kinetic models from the experimental data, respectively. The kinetic parameters and the coefficient of determination (R^2) of these models are evaluated and listed in Table 2. From the result of higher value of R^2 , it is indicated that the pseudo-second-order model was the best fit. A similar result was previously reported for the adsorption of MB onto ACC biocomposite films [30]. Therefore, the rate-controlling step in the adsorption process was chemisorption, involving valence forces through sharing or exchanging electrons between the adsorbent and the adsorbate.

TABLE 2: Kinetic parameters for methylene blue adsorption onto CPCN composite film.

Model	Parameters				R^2
	q_e (mg/g)	k_1 (l/mg)	q_e (mg/g)	k_2	
Pseudo-first-order	263.0	0.05			0.843
Pseudo-second-order			85.47	1.44×10^{-4}	0.989

TABLE 3: Adsorption capacity of various adsorbents to remove MB dye.

Adsorbent	Adsorbate	Adsorption capacity (mg/g)	Reference
Film (activated carbon +cellulose)	Methylene blue	103.66	[11]
NaIO ₄ - nanocellulose	Methylene blue	90.91	[40]
SDBS-modified ZSM-5	Methylene blue	15.68	[41]
Biofilms from palm date	Methylene blue	150.0	[42]
CPCN composite film	Methylene blue	63.13	This study

Consequently, the prepared CPCN composite film could be considered one of the biodegradable, nontoxic, and highly efficient adsorbents for removing cationic MB dye. The comparative study of the present CPCN composite film with others to remove MB dye from wastewater is shown in Table 3.

4. Conclusion

The CPCN composite film was successfully prepared via a blending method comprising chitosan, polyvinyl alcohol, and cornstarch, incorporating nanocellulose to develop an efficient adsorbent to remove methylene blue dye from wastewater. The prepared adsorbents were characterized using FTIR, SEM, and EDX characterization techniques before and after adsorption to understand their molecular interactions and surface morphology. The results of the above analysis convey evidence of the successful production of a composite film using chitosan, polyvinyl alcohol, and cornstarch with nanocellulose. The effect of pH, initial concentration of MB dye, dosage, and contact time on adsorption capacity of MB dye were studied batchwise and found a similar trend relating literature. For the maximum capacity of MB dye of 63.13 mg/g, the optimum parameters are a pH of 10, adsorbent dosage of 2 g, and initial dye concentration of 150 ppm with 12 min contact time. The adsorption equilibrium data were best fitted to the Langmuir isotherm model, implying that the models can be applied to remove MB dye of industrial wastewater by CPCN. The adsorption kinetic data were best fitted by the pseudo-second-order model for adsorption of MB using measured data by the prepared CPCN composite film. The findings of this study will help scale up the waste material (banana bracts) in the preparation of low-cost composite film-type adsorbents for the removal of organic dyes in the future.

Data Availability

All data generated through the experiments and analyzed during this study are included in this article.

Conflicts of Interest

The authors declare no conflict of interest.

Acknowledgments

All authors thank Research Cell (Project 2021-22), Jashore University of Science and Technology, for the financial support.

References

- [1] K. Li, J. Zhu, G. Guan, and H. Wu, "Preparation of chitosan-sodium alginate films through layer-by-layer assembly and ferulic acid crosslinking: Film properties, characterization, and formation mechanism," *International Journal of Biological Macromolecules*, vol. 122, pp. 485–492, 2019.
- [2] A. Mahieu, C. Terrié, and B. Youssef, "Thermoplastic starch films and thermoplastic starch/polycaprolactone blends with oxygen-scavenging properties: influence of water content," *Industrial Crops and Products*, vol. 72, pp. 192–199, 2015.
- [3] P. Suppakul, J. Miltz, K. Sonneveld, and S. W. Bigger, "Active packaging technologies with an emphasis on antimicrobial packaging and its applications," *Journal of Food Science*, vol. 68, no. 2, pp. 408–420, 2003.
- [4] K. Arshak, V. Velusamy, O. Korostynska, K. Oliwa-Stasiak, and C. Adley, "Conducting polymers and their applications to biosensors: emphasizing on foodborne pathogen detection," *IEEE Sensors Journal*, vol. 9, no. 12, pp. 1942–1951, 2009.
- [5] N. Yi and M. R. Abidian, "Conducting polymers and their biomedical applications," in *Biosynthetic Polymers for Medical Applications*, pp. 243–276, Woodhead Publishing, 2016.
- [6] F. Abbasi Ghaeni, G. Karimi, M. S. Mohsenzadeh, M. Nazarzadeh, V. S. Motamedshariaty, and S. A. Mohajeri, "Preparation of dual-template molecularly imprinted nanoparticles for organophosphate pesticides and their application as selective sorbents for water treatment," *Separation Science and Technology*, vol. 53, no. 16, pp. 2517–2526, 2018.
- [7] M. A. Syreina, S. I. Iatsunskyi, E. Coy et al., "Design of halloysite-based nanocomposites by electrospinning for water treatment," *Colloids and Surfaces A: Physicochemical and Engineering Aspects*, vol. 651, article 129696, 2022.

- [8] J. Meléndez-Marmolejo, L. Díaz de León-Martínez, V. Galván-Romero et al., "Design and application of molecularly imprinted polymers for adsorption and environmental assessment of anti-inflammatory drugs in wastewater samples," *Environmental Science and Pollution Research*, vol. 29, no. 30, pp. 45885–45902, 2022.
- [9] G. Z. Ke, K. D. Zhu, and Y. F. Li, "Structure and properties of chitosan and polyvinyl alcohol blend film," *Key Engineering Materials*, vol. 727, pp. 895–899, 2017.
- [10] S. Zivanovic, J. Li, P. M. Davidson, and K. Kit, "Physical, mechanical, and antibacterial properties of chitosan/PEO blend films," *Biomacromolecules*, vol. 8, no. 5, pp. 1505–1510, 2007.
- [11] W. Wang, B. Shan, L. Zhu, C. Xie, C. Liu, and F. Cui, "Anatase titania coated CNTs and sodium lignin sulfonate doped chitosan proton exchange membrane for DMFC application," *Carbohydrate Polymers*, vol. 187, pp. 35–42, 2018.
- [12] K. Wen, Y. Li, S. Zhang, X. Zhang, and R. Han, "Adsorption of Congo red from solution by iron doped PVA-chitosan composite film," *Desalination and Water Treatment*, vol. 187, pp. 378–389, 2020.
- [13] X. Tang and S. Alavi, "Recent advances in starch, polyvinyl alcohol based polymer blends, nanocomposites and their biodegradability," *Carbohydrate Polymers*, vol. 85, no. 1, pp. 7–16, 2011.
- [14] M. T. Islam, H. Jing, T. Yang et al., "Fullerene stabilized gold nanoparticles supported on titanium dioxide for enhanced photocatalytic degradation of methyl orange and catalytic reduction of 4-nitrophenol," *Journal of Environmental Chemical Engineering*, vol. 6, no. 4, pp. 3827–3836, 2018.
- [15] J. E. Padilla, J. Melendez, and L. A. Barrera et al., "High dispersions of carbon nanotubes on cotton-cellulose benzoate fibers with enhanced electrochemical generation of reactive oxygen species in water," *Journal of Environmental Chemical Engineering*, vol. 6, no. 1, pp. 1027–1032, 2018.
- [16] M. T. Islam, R. Saenz-Arana, H. Wang, R. Bernal, and J. C. Noveron, "Green synthesis of gold, silver, platinum, and palladium nanoparticles reduced and stabilized by sodium rhodizionate and their catalytic reduction of 4-nitrophenol and methyl orange," *New Journal of Chemistry*, vol. 42, no. 8, pp. 6472–6478, 2018.
- [17] M. T. Islam, J. E. Padilla, N. Dominguez et al., "Green synthesis of gold nanoparticles reduced and stabilized by squaric acid and supported on cellulose fibers for the catalytic reduction of 4-nitrophenol in water," *RSC Advances*, vol. 6, no. 94, pp. 91185–91191, 2016.
- [18] K. Amutha, A. Sudha, and D. Saravanan, "Characterization of natural fibers extracted from banana inflorescence bracts," *Journal of Natural Fibers*, vol. 19, no. 3, pp. 872–881, 2022.
- [19] S. R. Kanatt, M. S. Rao, S. P. Chawla, and A. Sharma, "Active chitosan-polyvinyl alcohol films with natural extracts," *Food Hydrocolloids*, vol. 29, no. 2, pp. 290–297, 2012.
- [20] S. M. Noorbakhsh-Soltani, M. M. Zerafat, and S. Sabbaghi, "A comparative study of gelatin and starch-based nano-composite films modified by nano-cellulose and chitosan for food packaging applications," *Carbohydrate Polymers*, vol. 189, pp. 48–55, 2018.
- [21] M. P. Indumathi, K. Saral Sarojini, and G. R. Rajarajeswari, "Antimicrobial and biodegradable chitosan/cellulose acetate phthalate/ZnO nano composite films with optimal oxygen permeability and hydrophobicity for extending the shelf life of black grape fruits," *International Journal of Biological Macromolecules*, vol. 132, pp. 1112–1120, 2019.
- [22] P. Zhou, Y. Luo, Z. Lv, X. Sun, Y. Tian, and X. Zhang, "Melt-processed poly (vinyl alcohol)/corn starch/nanocellulose composites with improved mechanical properties," *International Journal of Biological Macromolecules*, vol. 183, pp. 1903–1910, 2021.
- [23] P. K. Malik, "Dye removal from wastewater using activated carbon developed from sawdust: adsorption equilibrium and kinetics," *Journal of Hazardous Materials*, vol. 113, no. 1–3, pp. 81–88, 2004.
- [24] M. J. Alam, B. C. Das, M. W. Rahman, B. K. Biswas, and M. M. R. Khan, "Removal of dark blue-GL from wastewater using water hyacinth: a study of equilibrium adsorption isotherm," *Desalination and Water Treatment*, vol. 56, no. 6, pp. 1520–1525, 2015.
- [25] S. Parvin, M. W. Rahman, I. Saha, M. J. Alam, and M. M. R. Khan, "Coconut tree bark as a potential low-cost adsorbent for the removal of methylene blue from wastewater," *Desalination and Water Treatment*, vol. 146, no. 1, pp. 385–392, 2019.
- [26] M. Moniruzzaman, S. Kader, M. J. Alam, S. Aktar, A. Deb, and M. Khan, "Utilization of waste cigarette buds for the removal of reactive dye from wastewater," *Journal of Engineering Research and Application*, vol. 9, no. 2, pp. 2248–9622, 2019.
- [27] M. O. Rahman, M. A. Halim, A. Deb et al., "Modification of superabsorbent hydrogels for industrial wastewater treatment," *Advances in Polymer Technology*, vol. 2022, Article ID 8405230, 10 pages, 2022.
- [28] F. E. Titchou, R. A. Akbour, A. Assabbane, and M. Hamdani, "Removal of cationic dye from aqueous solution using Moroccan pozzolana as adsorbent: isotherms, kinetic studies, and application on real textile wastewater treatment," *Ground Water for Sustainable Development*, vol. 11, article 100405, 2020.
- [29] M. Mariano, N. E. Kissi, and A. Dufresne, "Cellulose nanocrystals and related nanocomposites: review of some properties and challenges," *Journal of Polymer Science, Part B: Polymer Physics*, vol. 52, no. 12, pp. 791–806, 2014.
- [30] N. Somsesta, V. Sricharoenchaikulb, and D. Aht-Onga, "Adsorption removal of methylene blue onto activated carbon/cellulose biocomposite films: equilibrium and kinetic studies," *Materials Chemistry and Physics*, vol. 240, article 122221, 2020.
- [31] A. Salama, H. A. Aljohani, and K. R. Shoueir, "Oxidized cellulose reinforced silica gel: new hybrid for dye adsorption," *Materials Letters*, vol. 230, pp. 293–296, 2018.
- [32] D. Pathania, S. Sharma, and P. Singh, "Removal of methylene blue by adsorption onto activated carbon developed from Ficus carica bast," *Arabian Journal of Chemistry*, vol. 10, Supplement 1, pp. S1445–S1451, 2017.
- [33] P. K. Malik, "Use of activated carbons prepared from sawdust and rice-husk for adsorption of acid dyes: a case study of Acid Yellow 36," *Dyes and Pigments*, vol. 56, no. 3, pp. 239–249, 2003.
- [34] A. I. Adeogun, E. A. Ofudje, M. A. Idowu, S. O. Kareem, and S. V. Babu, "Biowaste-derived hydroxyapatite for effective removal of reactive yellow 4 dye: equilibrium, kinetic, and thermodynamic studies," *ACS Omega*, vol. 3, no. 2, pp. 1991–2000, 2018.
- [35] E. Metcalf, *Wastewater Engineering: Treatment and Reuse*, McGraw Hill, New York, USA, 4th edition, 2003.

- [36] Y. S. Ho and G. McKay, "Kinetic models for the sorption of dye from aqueous solution by wood," *Process Safety and Environmental Protection*, vol. 76, no. 2, pp. 183–191, 1998.
- [37] M. W. Rahman, M. Y. Ali, I. Saha et al., "Date palm fiber as a potential low-cost adsorbent to uptake chromium (VI) from industrial wastewater," *Desalination and Water Treatment*, vol. 88, pp. 169–178, 2017.
- [38] M. Y. Ali, M. W. Rahman, M. Moniruzzaman et al., "Nypa fruticans as a potential low cost adsorbent to uptake heavy metals from industrial wastewater," *Indian Journal of Applied Business and Economic Research*, vol. 14, no. 2, pp. 1359–1371, 2016.
- [39] M. O. Rahman, N. Rahman, G. M. F. Ahmed et al., "Synthesis and implication of grafted polymeric adsorbent for heavy metal removal," *SN Applied Sciences*, vol. 2, no. 6, article 1089, 2020.
- [40] H. T. Kara, S. T. Anshebo, F. K. Sabir, and G. A. Workineh, "Removal of methylene blue dye from wastewater using periodiated modified nanocellulose," *International Journal of Chemical Engineering*, vol. 2021, Article ID 9965452, 16 pages, 2021.
- [41] D. M. EL-Mekkawi, F. A. Ibrahim, and M. M. Selim, "Removal of methylene blue from water using zeolites prepared from Egyptian kaolins collected from different sources," *Journal of Environmental Chemical Engineering*, vol. 4, no. 2, pp. 1417–1422, 2016.
- [42] M. Pasichnyk, J. Gaálová, P. Minarik, M. Václavíková, and I. Melnyk, "Development of polyester filters with polymer nanocomposite active layer for effective dye filtration," *Scientific Reports*, vol. 12, no. 1, article 973, 2022.